

1 **On the formation of non-radioactive copper during the production**  
2 **of  $^{64}\text{Cu}$  via proton- and deuteron-induced nuclear reactions on**  
3 **enriched  $^{64}\text{Ni}$  targets**

4 Ferenc Szelecsényi<sup>1</sup>, Gideon F. Steyn<sup>2</sup>, Zoltán Kovács<sup>1</sup>

5 <sup>1</sup>*Cyclotron Application Department, Institute for Nuclear Research of the Hungarian Academy of*  
6 *Sciences, ATOMKI, 18/c Bem tér, H-4026 Debrecen, Hungary*

7 <sup>2</sup>*iThemba Laboratory for Accelerator Based Sciences, Faure, P.O. Box 722, 7129 Somerset West, South*  
8 *Africa*

9 **Abstract**

10 Routine production of  $^{64}\text{Cu}$  commonly exploits the  $^{64}\text{Ni}(p,n)$  or  $^{64}\text{Ni}(d,2n)$  reactions. Above specific  
11 threshold energies, however, non-radioactive  $^{63}\text{Cu}$  and/or  $^{65}\text{Cu}$  are also co-produced. The non-radioactive  
12 (cold) Cu can significantly decrease the specific activity (SA) of  $^{64}\text{Cu}$ -labelled radiopharmaceuticals.  
13 Based on nuclear model calculations for the formation of non-radioactive Cu isotopes, theoretical specific  
14 activities (TSA) for  $^{64}\text{Cu}$  were estimated. Reported current production methods, however, often yield SA  
15 values that are lower than the corresponding TSA predictions by more than an order of magnitude. Most  
16 of the non-radioactive Cu causing this has been found to originate from sources other than co-production,  
17 indicating that there is still significant potential for method improvement.

18 **Keywords**

19  $^{64}\text{Ni}$  target, proton and deuteron reactions, ALICE 2014 calculations, TENDL 2014 library, non-  
20 radioactive Cu formation, specific activity of  $^{64}\text{Cu}$

21 **Introduction**

22 The production of radionuclides in high specific activity form, especially for application in positron  
23 emission tomography (PET) and targeted radiotherapy, is a continuous challenge for many laboratories.  
24 The desired radioisotopes would usually be contaminated to some degree, not only with other unwanted

25 radionuclides but with stable nuclides as well. With properly selected targetry, irradiation conditions and  
26 methods for preparation, separation, and labelling, however, both the radioactive and stable  
27 contaminations can often be decreased to acceptable levels.

28 The unique decay properties of the radionuclide  $^{64}\text{Cu}$  ( $T_{1/2} = 12.7$  h) make it useful for both imaging and  
29 therapy [1–3]. Two nuclear reactions have been suggested for its production with a radionuclidic purity  
30 sufficient for biomolecule labelling, namely  $^{64}\text{Ni}(p,n)^{64}\text{Cu}$  ( $Q = -2.5$  MeV) and  $^{64}\text{Ni}(d,2n)^{64}\text{Cu}$  ( $Q = -4.7$   
31 MeV). By keeping the bombarding energies below the thresholds for  $^{61}\text{Cu}$  ( $T_{1/2} = 3.4$  h) production via the  
32  $^{64}\text{Ni}(p,4n)^{61}\text{Cu}$  ( $Q = -30.1$  MeV) and  $^{64}\text{Ni}(d,5n)^{61}\text{Cu}$  ( $Q = -32.3$  MeV) reactions, respectively, the only co-  
33 produced Cu contaminants are stable  $^{63}\text{Cu}$  and  $^{65}\text{Cu}$ . Note that  $^{62}\text{Cu}$  ( $T_{1/2} = 9.74$  m) is, in principle, also a  
34 potential contaminant but due to its relatively short half-life, its presence can be tolerated as it will decay  
35 to an acceptably low level after a relatively short waiting time post end of bombardment (EOB), for  
36 example during the typical chemical separation time. Commercial medical cyclotrons with typical energy  
37 capability, *e.g.* 30/15 or 18/9 MeV for protons/deuterons, are therefore ideal for this purpose. There are  
38 still some concerns, however, about the presence of non-radioactive Cu in final product solutions [2–4].

39 Several authors developed  $^{64}\text{Cu}$  production systems based on proton activation of highly enriched  $^{64}\text{Ni}$   
40 targets, and reported measured SA values [2–5]. In order to critically evaluate these SA values, we felt  
41 there was a need to compare them with corresponding theoretical specific activity (TSA) predictions as  
42 well as with the theoretical maximum specific activity (TMSA) of the relevant nuclear reactions. No  
43 measured SA values could be found in the literature for the deuteron-based production route however  
44 TSA and TMSA values for deuterons can provide a valuable comparison with the proton-based  
45 production route.

46 The relevant reactions for the co-production of the stable Cu radionuclides are  $^{64}\text{Ni}(p,2n)^{63}\text{Cu}$  ( $Q = -10.4$   
47 MeV),  $^{64}\text{Ni}(d,3n)^{63}\text{Cu}$  ( $Q = -12.6$  MeV) and  $^{64}\text{Ni}(d,n)^{65}\text{Cu}$  ( $Q = +5.2$  MeV). In principle, the  $^{64}\text{Ni}(p,\gamma)^{65}\text{Cu}$   
48 reaction channel is always open in the proton energy region of interest, however, the cross sections for  
49 formation of  $^{65}\text{Cu}$  via this reaction is well below 1 mb, therefore its contribution is negligible. In the case  
50 of deuterons, however, the  $^{64}\text{Ni}(d,n)^{65}\text{Cu}$  reaction channel is always open in any production energy  
51 window due to its positive  $Q$ -value. As its excitation function is expected to reach a maximum of several  
52 hundred millibarn, which is typical for (d,n) reactions in that mass region, its contribution to stable copper  
53 formation cannot be neglected.

54 The basic aim of this study was to estimate the level of stable Cu contamination(s) from co-production in  
55 typical energy windows for both the proton-based and deuteron-based production routes, using yield  
56 predictions derived from the formation cross sections according to the TENDL 2014 nuclear data library

57 [6,7] and the ALICE 2014 nuclear model code [8]. It should be noted that the theoretical excitation  
58 functions of non-radioactive nuclides remain *inter alia* untested against experimental measurements.  
59 Thus, in order to get an idea of the typical predictive power of these codes for the relevant reactions, in  
60 the energy region up to about 30 MeV, comparisons with measured data for similar reactions in a wider  
61 mass region ( $40 \leq A \leq 130$ ) have also been performed.

## 62       **Theoretical calculations**

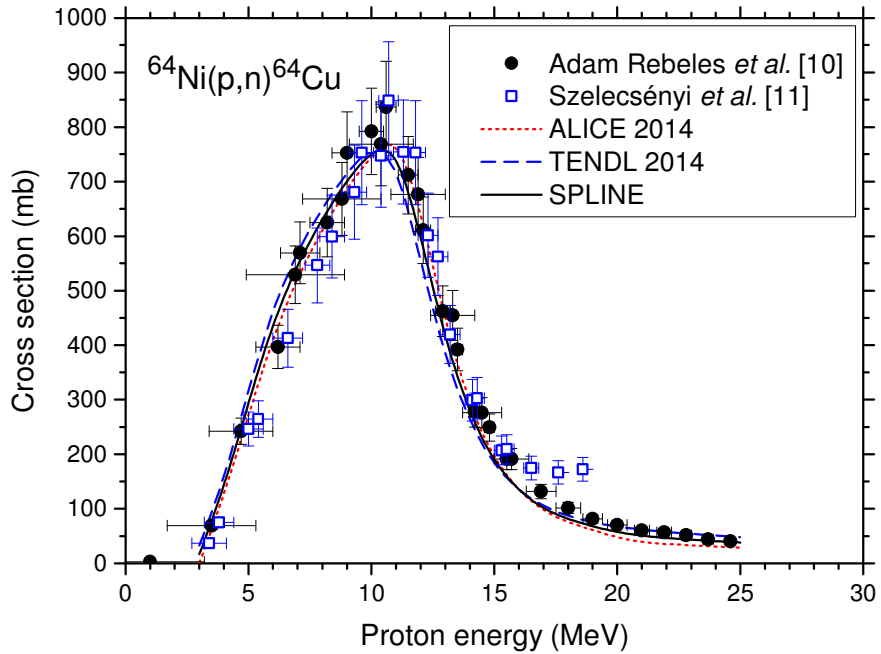
63 Production yields for  $^{63}\text{Cu}$  and  $^{65}\text{Cu}$  have been calculated by deriving their excitation functions using  
64 nuclear model calculations, as measured cross-section data for these stable nuclides do not exist. For the  
65 non-radioactive Cu,  $^{64}\text{Cu}$  and several other nuclides produced by similar reactions, predictions by means  
66 of the TALYS code [6], according to the TALYS-based evaluated nuclear data library TENDL 2014 [7],  
67 as well as the ALICE 2014 code system [8] have been employed. The ALICE 2014 code was consistently  
68 used with default parameters and no “fine tuning” of any parameters was performed. The objective was to  
69 look for order-of-magnitude predictions by observing the typical level of agreement by both TENDL  
70 2014 and ALICE 2014 (using mainly default parameters) with experimental data, where available, in the  
71 relevant mass and energy regions, rather than to search for the most fine-tuned calculations in terms of  
72 completeness and/or accuracy that might be possible today. The default parameter choice selects the  
73 Hybrid Monte Carlo Simulation (HMS) precompound decay model of Blann [9] in conjunction with the  
74 Weiskopf-Ewing evaporation model for the subsequent decay of an equilibrated nuclear system.  
75 Precompound emission of d, t,  $^3\text{He}$  and  $^7\text{Be}$  clusters in addition to n, p and  $\alpha$ -particles was selected. An  
76 energy mesh size of 0.2 MeV was specified and 100 000 cascade events were performed at each incident  
77 energy.

## 78       **Results and discussion**

### 79       **Cross sections of proton-induced reactions**

80 First, the prediction capabilities of the model codes in the case of the  $^{64}\text{Ni}(p,n)^{64}\text{Cu}$  nuclear reaction, for  
81 which good experimental data exist, were checked. The results are shown in Fig. 1. Good overall  
82 agreement between the most recent experimental data of Adam Rebeles *et al.* [10] and Szelecsényi *et al.*  
83 [11], the TENDL 2014 compilation and the ALICE 2014 calculations is evident. Next, the predicted  
84 excitation functions for stable  $^{63}\text{Cu}$  via the  $^{64}\text{Ni}(p,2n)^{63}\text{Cu}$  reaction are shown in Fig. 2. In this case, the  
85 agreement is also acceptable although ALICE 2014 predicts a somewhat higher value at the peak  
86 maximum, which is also shifted towards higher energies. As will be explained in more detail later, spline

87 fits through the mean values of the two sets of theoretical predictions reproduce the excitation functions  
 88 of various (p,n) and (p,2n) reactions quite well up to 30 MeV. (The spline fits were performed with the  
 89 well-known graphing software package Origin 9.1, by selecting either the B-spline or Akima spline  
 90 options built into the code.) The same applies to the relevant deuteron-induced reactions. Figures 1 and 2  
 91 also include these spline-fit curves.

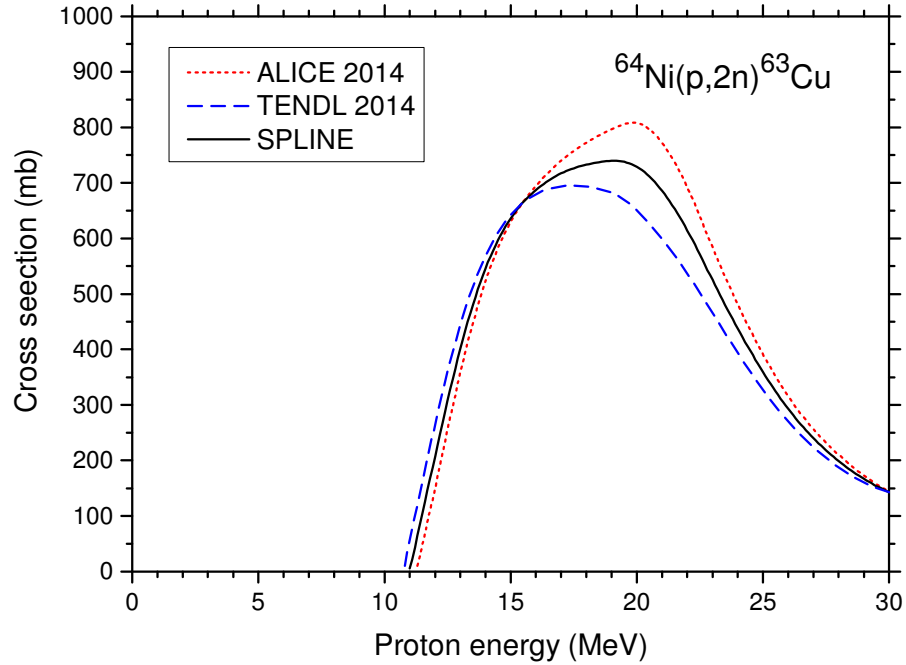


92

93 **Fig. 1.** Excitation functions for the production of  $^{64}\text{Cu}$  in the bombardment of  $^{64}\text{Ni}$  with protons.

94 **Cross sections of deuteron-induced reactions**

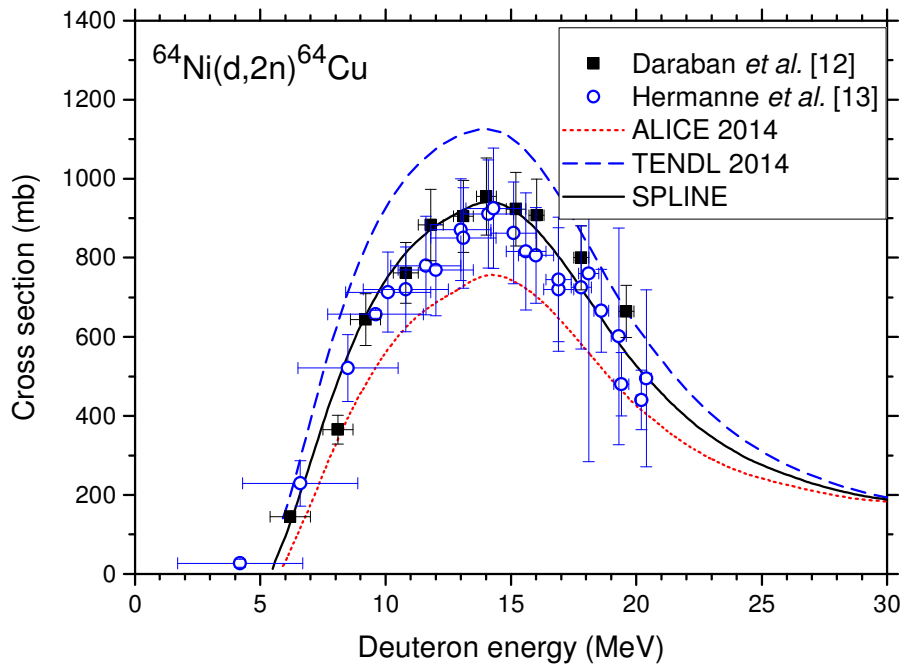
95 Based on the excitation-function results for the  $^{64}\text{Ni}+p$  reactions, we expected a similar tendency for  
 96  $^{64}\text{Ni}+d$  processes as well. Unfortunately, the ALICE 2014 and TENDL 2014 results exhibited larger  
 97 differences from each other (see Figs. 3, 4 and 5). Figure 3 shows the excitation functions for the  
 98 production of  $^{64}\text{Cu}$  in the deuteron bombardment of  $^{64}\text{Ni}$ . The TENDL 2014 values seem to overpredict  
 99 the most recent experimental data of Daraban *et al.* [12] and Hermanne *et al.* [13]. In contrast, an  
 100 underprediction is observable in the case of ALICE 2014. Interestingly, the spline fit through the mean  
 101 values reproduces the measured data quite well. Similar behavior was found for several other (d,2n)  
 102 reactions as well in the surrounding mass region. We would like to strongly state here that the adopted  
 103 fitting of mean values from the two sets of calculations is by no means advocated as a suitable approach  
 104 for general use. It merely seems to be a reasonable thing to do in this particular study as suitable  
 105 agreement with measured data for the relevant reactions is evident in this mass and energy region.



106

107 **Fig. 2.** Excitation functions for the production of  $^{63}\text{Cu}$  in the bombardment of  $^{64}\text{Ni}$  with protons.

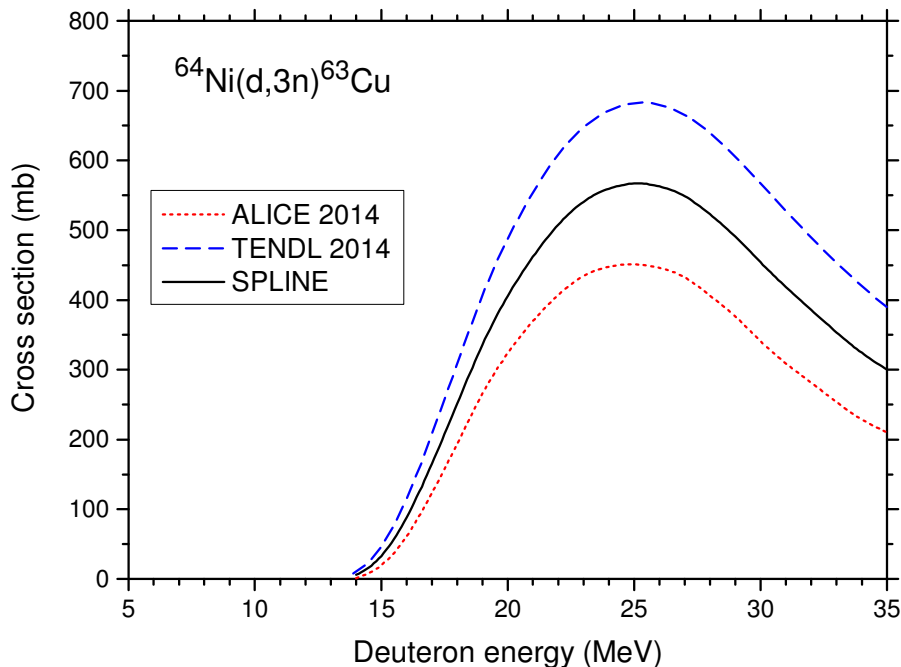
108



109

110 **Fig. 3.** Excitation functions for the production of  $^{64}\text{Cu}$  in the bombardment of  $^{64}\text{Ni}$  with deuterons.

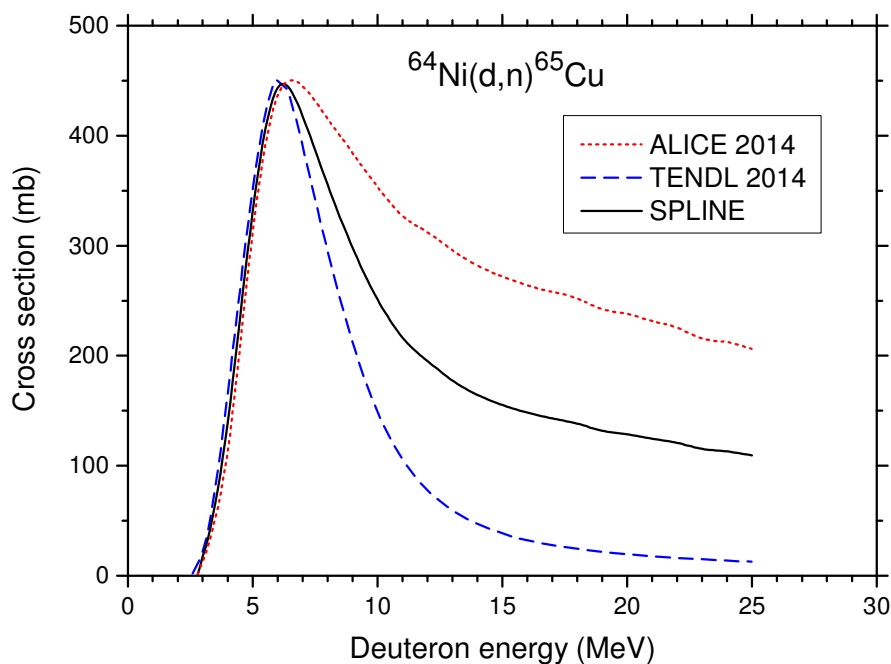
111 The excitation-function predictions for the formation of stable  $^{63}\text{Cu}$  in the deuteron bombardment of  $^{64}\text{Ni}$   
 112 are shown in Fig. 4. Once again, the TENDL 2014 values are higher than the ALICE 2014 values. This  
 113 was found to be a prevalent feature for various (d,2n) and (d,3n) reactions in the  $40 \leq A \leq 130$  mass  
 114 region. In the cases of the  $^{89}\text{Y}(d,2n)^{89}\text{Zr}$  and  $^{89}\text{Y}(d,3n)^{88}\text{Zr}$  reactions, for example, it was found that the  
 115 spline fits reproduced the relevant experimental data [14,15,16] to the same level of agreement as  
 116 exhibited in Fig. 3. In fact, not a single complete set of experimental excitation-function data that  
 117 included the (d,n), (d,2n), and (d,3n) reactions on the same nucleus in the  $40 \leq A \leq 130$  mass region was  
 118 found in EXFOR [17]. This is because, invariably, some of the product nuclei are stable. Several cases  
 119 were found, however, where data existed for two of the reactions. Unfortunately, space limitations  
 120 preclude an in-depth discussion of all those results here. It was found, however, that the spline fits  
 121 generally reproduce the data satisfactorily up to 30 MeV.



122  
 123 **Fig. 4.** Excitation functions for the production of  $^{63}\text{Cu}$  in the bombardment of  $^{64}\text{Ni}$  with deuterons.

124 A rather different trend has been observed for the (d,n) reactions. The predictions for the  $^{64}\text{Ni}(d,n)^{65}\text{Cu}$   
 125 reaction (see Fig. 5) show the opposite trend beyond the peak region, namely that the ALICE 2014 values  
 126 exhibit a probable overprediction and the TENDL 2014 values a probable underprediction. Up to the peak  
 127 maximum, however, the agreement is generally good. Concerning the (d,n) reaction, it should be pointed  
 128 out that experimental data on naturally mono-isotopic nuclei and/or nuclei with large natural abundances  
 129 are quite sparse. The reason is because this reaction very often leads to another stable nucleus. In addition,

130 a significant fraction of the published cross sections compiled in EXFOR [17] only cover the low energy  
 131 region (*i.e.* near the threshold or not significantly beyond the peak maximum). Nevertheless, in nine data  
 132 sets found (leading via the (d,n) reaction to  $^{48}\text{V}$ ,  $^{55}\text{Co}$ ,  $^{59}\text{Cu}$ ,  $^{67}\text{Ga}$ ,  $^{71}\text{As}$ ,  $^{75}\text{Br}$ ,  $^{79}\text{Rb}$ ,  $^{95g}\text{Tc}$  and  $^{123}\text{I}$ ) the  
 133 TENDL 2014 and ALICE 2014 values exhibit the same trend as in Fig. 5, with ALICE clearly  
 134 overpredicting and TENDL clearly underpredicting the measured data beyond the peak region. Also, the  
 135 spline fits through the mean values give a reasonable estimate of the peak region up to the onset of the  
 136 high-energy plateau, making them useful for this study. Figure 6 shows the excitation function of the  
 137  $^{47}\text{Ti}(d,n)^{48}\text{V}$  reaction as an example to illustrate this. Consequently, the decision was made to adopt these  
 138 spline fits for purposes of calculating the integral yield predictions for  $^{63,64,65}\text{Cu}$ , from which TSA and  
 139 TMSA values could be derived.



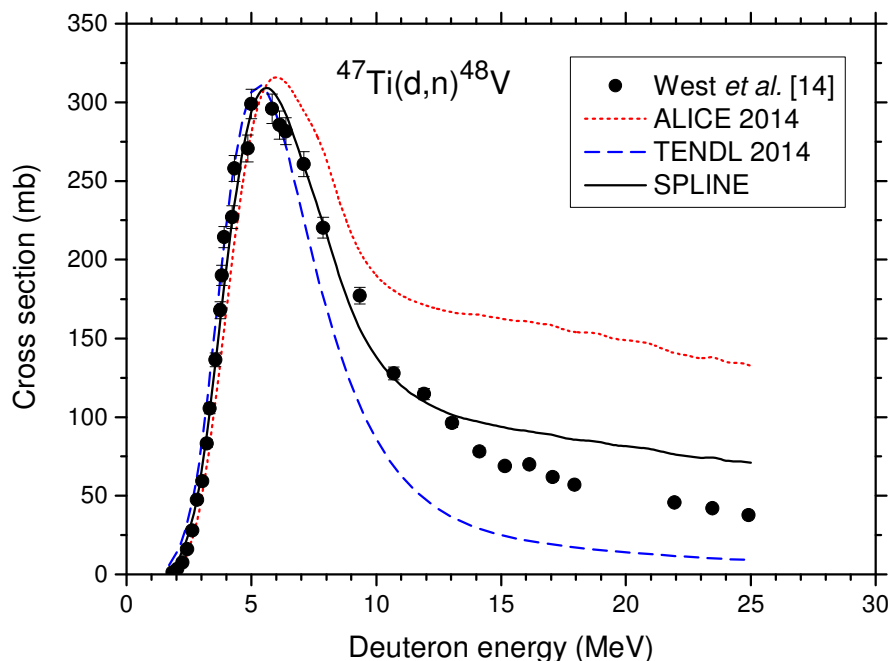
140

141 **Fig. 5.** Excitation functions for the production of  $^{65}\text{Cu}$  in the bombardment of  $^{64}\text{Ni}$  with deuterons.

142 **Yield and TSA calculations**

143  $^{64}\text{Ni}+p$  reactions

144 Based on the spline fits of the cross sections for the  $^{64}\text{Ni}(p,n)^{64}\text{Cu}$  and the  $^{64}\text{Ni}(p,2n)^{63}\text{Cu}$  reactions, we  
 145 calculated the absolute number of nuclei produced of each Cu species per unit charge (*i.e.* physical  
 146 number yield of nuclei/Coulomb – see Fig. 7) as well as the corresponding TSA values, as a function of  
 147 the bombarding energy. It is evident that above 10 MeV the number of  $^{63}\text{Cu}$  nuclei increases sharply and



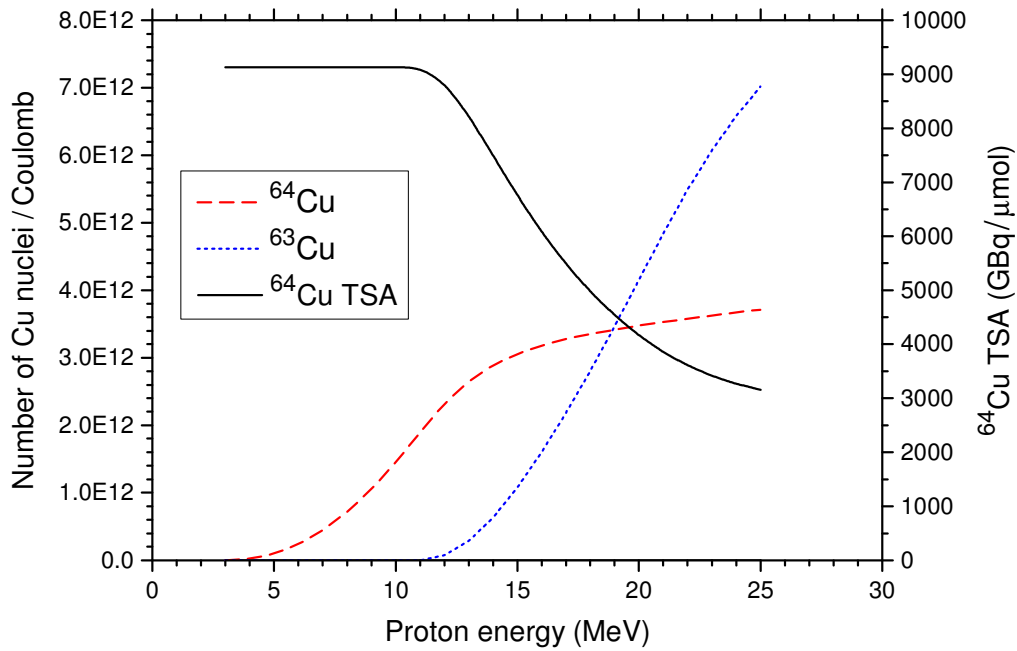
148

149 **Fig. 6.** Excitation functions for the production of  $^{48}\text{V}$  in the bombardment of  $^{47}\text{Ti}$  with deuterons.

150 almost the same amount of  $^{63}\text{Cu}$  and  $^{64}\text{Cu}$  nuclei are formed already at 19 MeV. Consequently, the TSA  
 151 value at 19 MeV is only about 50% of the TMSA value of 9130 GBq/ $\mu\text{mol}$  ( $1.43 \times 10^{17}$  Bq/g). Taking  
 152 into account the decay of  $^{64}\text{Cu}$  during longer activations, the actual SA values will in practice always be  
 153 lower than the corresponding TSA values. The TSA reaches the TMSA value below the formation  
 154 threshold of  $^{63}\text{Cu}$ , the latter value of which is always a physical upper limit. Naturally, the separation,  
 155 labelling and transportation times also lead to a decrease in the SA available for biomolecule labelling.

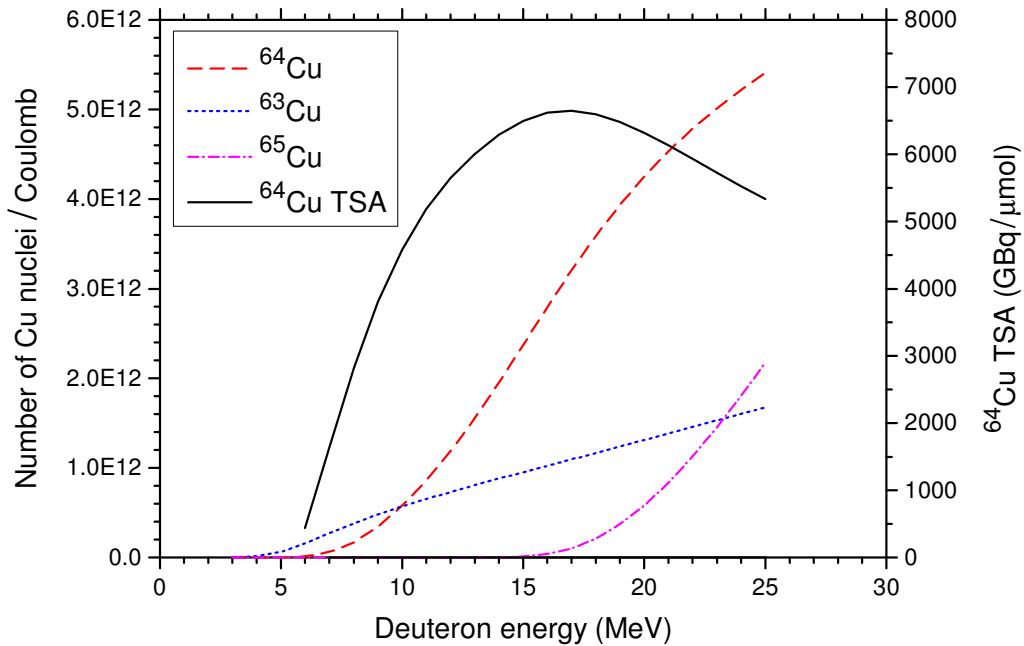
156  $^{64}\text{Ni}+d$  reactions

157 Due to the inevitable co-formation of  $^{65}\text{Cu}$  in  $^{64}\text{Ni}+d$  reactions, the  $^{64}\text{Cu}$  cannot be produced in non-  
 158 radioactive copper contamination-free form in the whole investigated energy region, as shown in Fig. 8.  
 159 The contamination ratio reaches its minimum at about 17 MeV, where the TSA curve reaches a peak  
 160 maximum (*i.e.* the TMSA value) of 6648 GBq/ $\mu\text{mol}$  ( $1.04 \times 10^{17}$  Bq/g). Unfortunately, the majority of  
 161 hospital-based accelerators are capable of accelerating deuterons only up to 9 MeV, therefore only about  
 162 57% of TMSA (*i.e.* 3846 GBq/ $\mu\text{mol}$  or  $6.02 \times 10^{16}$  Bq/g) is theoretically available on such machines.  
 163 Similar to the (p,n) production route, the contamination level increases with increasing irradiation time  
 164 and practical SA values are correspondingly lower. It is also interesting to note that the TMSA value of  
 165 the (d,2n) reaction was found to be lower, estimated to be 72.8% of the TMSA value of the (p,n) reaction.



166

167 **Fig. 7.** Absolute number of  $^{63}\text{Cu}$  and  $^{64}\text{Cu}$  nuclei produced per unit charge, as well as the corresponding  
 168  $^{64}\text{Cu}$  theoretical specific activity (TSA), as a function of proton energy.



169

170 **Fig. 8.** Absolute number of  $^{63}\text{Cu}$ ,  $^{64}\text{Cu}$  and  $^{65}\text{Cu}$  nuclei produced per unit charge, as well as the  
 171 corresponding  $^{64}\text{Cu}$  theoretical specific activity (TSA), as a function of deuteron energy.

## 172 Comparison with measured specific activities

173 Table 1 presents some measured SA values for  $^{64}\text{Cu}$  productions utilizing highly enriched  $^{64}\text{Ni}$  (> 95%)  
 174 electroplated onto gold backings and irradiated with protons. During bombardment the gold backings are  
 175 cooled with water. Although there are many differences in the details of the targetry, *e.g.* target layer  
 176 thickness and diameter, backing thickness and methods of preparation, other target holder materials,  
 177 cooling geometry, etc., it is nevertheless interesting to compare these SA values with the corresponding  
 178 TSA values.

179 As can be seen from Table 1, only one group activated their samples with an energy (15.5 MeV) that is  
 180 higher than the threshold of the  $^{64}\text{Ni}(p,2n)^{63}\text{Cu}$  reaction [2]. At this energy, the expected TSA would be  
 181 6412 GBq/ $\mu\text{mol}$ , which is more than an order of magnitude higher than most of the results presented by  
 182 those authors. The best result reported by McCarthy *et al.* [2] is a SA value at EOB which is still more  
 183 than a factor of 8 lower than the corresponding TSA value (734 GBq/ $\mu\text{mol}$ ). The high amount of total Cu  
 184 prompted further investigations into the detail of possible sources of non-radioactive Cu. This group  
 185 pointed out that cleaning the targets after irradiation (with 1.0 N  $\text{HNO}_3$ , Milli-Q water, hexane and with  
 186 ethanol) dramatically increases (up to twenty times) the SA. They found that the cooling media could  
 187 always be a major source of non-radioactive Cu. Additionally, targets prepared from re-used  $^{64}\text{Ni}$  material  
 188 produced higher SA than targets prepared from new material. This is a very significant finding and can be  
 189 explained by the fact that previous separation chemistry purified the target material from its initial non-  
 190 radioactive Cu content. It was also shown that the chemical separation can release Cu contaminants from  
 191 the gold backings.

192 **Table 1.** Reported specific activities in  $^{64}\text{Cu}$  productions using targets of highly enriched  $^{64}\text{Ni}$  (> 95%)  
 193 electroplated onto gold backings.

Incident energy (MeV)	Bombardment time	SA at EOB* (GBq/ $\mu\text{mol}$ )	TSA (GBq/ $\mu\text{mol}$ )	Reference
15.5	2–3 h	223–734	6412	McCarthy <i>et al.</i> [2]
10	2–3 h	861–1685	9130	Thieme <i>et al.</i> [3]
11.7	100–120 min	13.1– 28.9	9130	Jeffery <i>et al.</i> [4]
11.1	Not given	977– 2021	9130	Walther <i>et al.</i> [5]

194 \*Minimum and maximum SA values reported by these authors.

195 Thieme *et al.* [3] and Walther *et al.* [5] reported on a positive effect on the SA by using thinner gold  
 196 backings (in fact, gold foils on Al backings). The latter group also investigated Pt backings but those  
 197 results showed similar SA values to the targets with Au backings. Both groups also reported best results

198 where the SA values significantly exceed 1.5 TBq/ $\mu$ mol. They also reported that further investigation is  
199 ongoing and that there is potential for improvement. Based on the findings of this study it seems that  
200 these groups are on the right track.

201 An important finding by Jeffery *et al.* [4] is that not only non-radioactive Cu is problematic but that other  
202 non-radioactive metals are also accumulating with successive irradiation and recycling of the target  
203 material. They concluded that future work should focus on refining the  $^{64}\text{Ni}$  recycling process.

204 Admittedly, the uncertainties in the TSA and TMSA predictions may be significant and their assessment  
205 with a very high level of confidence does not appear feasible in the context of the present study. It is  
206 unlikely, however, that such uncertainties will significantly exceed the overall level of disagreement  
207 between integrated yields derived from the nuclear model calculations as compared to the corresponding  
208 yields derived directly from spline fits through the experimental excitation-function data. Observed  
209 differences do not exceed 30%, which is significantly less than the differences observed between actual  
210 measured SA values and the corresponding TSA predictions (see Table 1). To conclude, it is worthwhile  
211 mentioning the conclusion by Lapi *et al.* [18] that progress over the last 30 years on obtaining high  
212 specific activity radionuclides and radiopharmaceuticals is disappointing. While this particular statement  
213 was pertaining more to  $^{11}\text{C}$  and  $^{18}\text{F}$  agents, the same is certainly true also for  $^{64}\text{Cu}$ , however, recent  
214 advances in the field are reassuring.

## 215 **Conclusion**

216 Based on theoretical predictions by means of the ALICE and TALYS codes,  $^{64,63}\text{Cu}$  and  $^{65,64,63}\text{Cu}$  physical  
217 yields were calculated for the  $^{64}\text{Ni}+p$  and  $^{64}\text{Ni}+d$  reactions, respectively. For both reactions the formation  
218 of non-radioactive  $^{63}\text{Cu}$  (above 10 and 13 MeV, respectively) significantly decreases the SA of the final  
219  $^{64}\text{Cu}$  product. In addition, the deuteron-based route always co-produces stable  $^{65}\text{Cu}$  together with the  $^{64}\text{Cu}$   
220 regardless of the selected energy window. For this reason, the TMSA value for  $^{64}\text{Cu}$  obtained from a  
221 proton-based production route is higher than for a deuteron-based production route. Nevertheless, a more  
222 important consideration for any production system is to constrain the amount of non-radioactive Cu from  
223 sources other than co-production. While progress has clearly been made in recent years, further  
224 experimental work is necessary to reach higher SA values, which is important for increasing the  
225 effectiveness of receptor binding studies.

## 226 **Acknowledgements**

227 The Hungarian authors wish to thank the financial support by the Hungarian Research Foundation,  
228 (Budapest, OTKA K108669).

229        **References**

- 230    1. Qaim SM (2015) *J Radioanal Nucl Chem*, DOI 10.1007/s10967-014-3923-2 (published online, in  
231        press) and references therein
- 232    2. McCarthy DW, Shefer RE, Klinkowstein RE, Bass LA, Margeneau WH, Cutler CS, Anderson CJ,  
233        Welch MJ (1997) *Nucl Med Biol* 24:35–43
- 234    3. Thieme S, Walther M, Pietzsch H-J, Henniger J, Preusche S, Mading P, Steinbach J (2012) *Appl*  
235        *Radiat Isot* 70:602–608
- 236    4. Jeffery CM, Smith SV, Asad AH, Chan S, Price RI (2012) *AIP Conf. Proc.* 1509:84–90
- 237    5. Walther M, Preusche S, Fuechtner F, Pietzsch HJ, Steinbach J (2012) *AIP Conf. Proc.* 1509:81–83
- 238    6. Koning AJ, Rochman D (2012) *Nuclear Data Sheets* 113:2841–2934
- 239    7. Koning AJ, Rochman D, van der Marck D, Kopecky SJ, Sublet JCh, Pomp S, Sjöstrand H, Forrest R,  
240        Bauge E, Henriksson H, Cabellos O, Goriely S, Leppanen J, Leeb H, Plompen A, Mills R (2014)  
241        TENDL 2014: TALYS-based evaluated nuclear data library, available from [www.talys.eu](http://www.talys.eu)
- 242    8. Blann M, Konobeev AY, Wilson WB, Mashnik SG, Manual for Code Alice, July 2008; ALICE 2014:  
243        RSICC Code Package PSR-550, available from <https://rsicc.ornl.gov>
- 244    9. Blann M (1996) *Phys Rev C* 54:1341–1349
- 245    10. Adam Rebeles R, van den Winkel P, Hermanne A, Tárkányi F (2009) *Nucl Instr and Meth. B*  
246        267:457–461
- 247    11. Szelecsényi F, Blessing G, Qaim SM (1993) *Appl Radiat Isot* 44: 575–580
- 248    12. Daraban L, Adam Rebeles R, Hermanne A (2009) *Appl Radiat Isot* 67:506–510
- 249    13. Hermanne A, Tárkányi F, Takács S, Kovalev SF, Ignatyuk A (2007) *Nucl Instr and Meth B* 258:308–  
250        312
- 251    14. West HI, Lanier RG, Mustafa MG, Nuckolls RM, Nagle RJ, O'Brien H (1993) Report UCRL-ID-  
252        115738 (1993) p 3-1–3-17
- 253    15. Uddin MS, Baba M, Hagiwara M, Tárkányi F, Ditrói F (2007) *Radiochim Acta* 95 187–192
- 254    16. Tárkányi F, Ditrói F, Takács S, Csikai J, Mahunka I, Uddin MS, Hagiwara M, Baba M, Ido T,  
255        Hermanne A, Sonck M, Shubin Yu, Dityuk AI (2005) *AIP Conf. Proc.* 769:1658–1661
- 256    17. Experimental Nuclear Reaction Data Library (EXFOR), Database Version of March 16, 2015,  
257        available from <http://www-nds.iaea.org>
- 258    18. Lapi SE, Welch MJ (2013) *Nucl Med Biol* 40:314–320